

## REMARKS

By the present amendment, claim 1 has been amended. Claims 3 and 12 have been cancelled. Claims 1, 7-10, 13-14, and 16-20 are currently pending in the application.

The Examiner has maintained the rejection to the drawing in spite of evidence provided by applicant that the drawing conforms to industry standards. Without any reason, the Examiner has declared the Neblette's drawing irrelevant. The Examiner is requested to provide evidence beyond personal opinion as to why applicant's drawing is improper. Applicant maintains that the drawing is proper and would be understood by those of ordinary skill in the art.

Claims 1, 3, 7-8, and 16-20 were rejected under 35 U.S.C. 103 as being unpatentable over the combination of EP 1220026, U.S. Patent No. 4,332,889 to Siga et al., and U.S. Patent No. 5,698,380 to Toya.

The limitations of claim 12 have been incorporated into current claim 1. Since this rejection does not include claim 12, it is respectfully submitted that this rejection has been overcome.

Claim 16 was rejected over the combination of EP '026 in view of Siga et al and further in view of Tsuzuki.

Claim 14 was rejected over the combination of EP '026 in view of Siga et al and further in view of Goto or Farid.

Claims 10 and 19-20 were rejection over the combination of EP '026 in view of Siga et al and further in view of Toya.

None of these three rejections includes claim 12, the limitations of which have been incorporated into claim 1. Thus it is submitted that these rejections have been overcome.

Further, a declaration under 37 C.F.R. 1.132 is submitted herewith. This declaration shows the unexpected results obtained by using silver iodide over silver iodobromide. Oyamada does not describe the high silver iodide content of from 90 to 100 mol. %, nor the photosensitive silver halide having an average  $\gamma$ -phase ratio in a range from 5 to 90 mol. %. Although Oyamada specifically describes  $\text{AgI}=3.5$  mol.%, the declaration shows that high silver iodide content provides unexpected results such as acceleration of development and improvements in color difference depending on developing time and color tone preservability, which effects cannot be obtained with  $\text{AgI}=3.5$  mole, based on the comparative test results shown in Table 1 of the declaration.

Similarly, Toya (US 5698380), Toya (US 5998126), Yoshioka (EP 1220026) and Tsuzuki (US 5677121), provide no suggestion of the above-described unexpected results of the high  $\text{AgI}$  content of the present invention. Photothermographic materials in the prior art with high  $\text{AgI}$  content had a problem of significant suppression of development due to  $\text{AgI}$ . However, the present inventor first discovered that reducing the amount of silver in the high  $\text{AgI}$  content rapidly increases development progression. This cannot be determined from Toya (US 5998126, 5698380) and Yoshioka (EP 1096310) wherein  $\text{AgBr}$  is used. Further, the unexpected results of the present invention cannot be obtained from the amount of silver in the coating as described in the Examples of Toya and Yoshioka. Therefore, the combination of references does not teach or suggest that

coating silver in amounts far less than those used for silver bromide or silver iodobromide is effective.

Further, although the Office action takes the position that silver iodide of 90 mole to 100 mole% is obvious in view of the teaching of silver iodide of 3.5 mole%, there is a critical difference between the high silver iodide content comprising pure silver iodide or substantially pure silver iodide and silver iodobromide with a low iodide content.

As described in the accompanying excerpt from The Theory of the Photographic Process, Fourth Edition, T. H. James, 1977, Macmillan Publishing Co., Inc., AgBr and AgCl have a rock salt structure. In contrast AgI is crystallized in either the hexagonal, wurtzite structure ( $\beta$ -AgI) or in the cubic zinc blende structure ( $\gamma$ -AgI) (pp. 1-2). AgBr and AgCl can exist in all proportions in solid solutions, whereas only limited amounts of solid solution can occur between AgBr and AgI. When the amount of iodine is low, AgI is incorporated in the rock salt structure of AgBr. When the amount of iodine is high, only a small amount of AgBr is incorporated in the structure of  $\beta$ - or  $\gamma$ -AgI or AgBr is present as a separate phase (pp. 3-4). There is a marked difference between optical characteristics of AgBrI with low iodide content and that of AgI as set forth on pp. 39-41.

Thus, it can be seen that there are large differences in the crystallographic, thermodynamic, optical, and electronic properties, as well as in photographic response between high AgI content material and silver iodobromide with low iodine content. Therefore, although there are descriptions of silver iodobromide and the like in Examples of low iodine content and general descriptions set forth in the specifications of the cited references, high and low iodine content materials are not obvious variants.

Claims 1, 3, 7-10, and 12-20 were rejected under 35 U.S.C. 103 as being anticipated by U.S. Patent No. 6,143,488 to Uytterhoeven et al. in view of EP 01096310 (EP '310). Uytterhoeven does not explicitly describe the amount of silver in the coating either in the specification or the Examples. Therefore, the amount of silver has been calculated based on the formulation described in Examples.

US 6143488 (Uytterhoeven) Example 1:

First, the amount of AgI in the coating is determined:

10.7 % silver behenate (MW = 448) in 4g of silver behenate dispersion  
 $= 4 \times 0.107 / 448 = 9.6 \times 10^{-4} \text{ mole.}$  ... (1)

0.72 g of PC03 ... 8 mol. % with respect to silver behenate ... (2)

0.16 g of phthalazine

0.74 g of reducing agent (LOWINOX<sup>TM</sup>)

1.2 g of MEK

Total 6.82 g = 6.82 cc (when specific gravity is 1) ... (3)

Coating is carried out at a wet coating thickness of 80  $\mu\text{m}$  ( $80 \times 10^{-6} \text{ m}^3$  per  $1 \text{ m}^2$ )  
 $= 80 \text{ cc/m}^2$  ... (4)

From (1), (3) and (4), the amount of silver in the coating is:

$$9.6 \times 10^{-4} \times 108 \text{ (MW of Ag)} \times 80/6.82 = 1.22 \text{ g/m}^2.$$

From (2), the iodine compound PC03 is 8 mol. % with respect to silver.

The amount of silver of AgI in the coating =  $1.22 \text{ g/m}^2 \times 8 \% \approx 0.1 \text{ g/m}^2$ .

Therefore, the amount of silver of AgI in the coating calculated based on the formulation in the Examples of Uytterhoeven is substantially larger than the amount of

silver, 0.005 to 0.05 g/m<sup>2</sup>, of the photosensitive silver halide in the coating required by claim 1 of the present application.

Further, the formulation in the examples of Uytterhoeven is is-situ silver halide prepared by conversion, in contrast to the requirements set forth in claim 1. There is a substantial difference between organic silver salt dispersions prepared through conversion and those in which a photosensitive silver halide is formed in a state where the non-photosensitive organic salt is not present.

Organic silver salts are prepared through stages of: organic acid → alkali metal soap → organic silver salt. Among them, only the alkali metal soap is hydrophilic and is stably dispersible in water. The organic acid and the organic silver salt are highly hydrophobic and cannot be stably dispersed in water, and therefore need to be dispersed using an organic solvent. In contrast, silver halides that have been prepared in advance (preformed) are water dispersed using a hydrophilic colloid such as gelatin, and therefore are stably dispersible in water. The above explanation and Figures 1 and 2 (below) illustrate conditions of dispersion of a silver halide and an organic silver salt in an image forming layer.

Figure 1 shows a dispersion obtained by the process in which a preformed silver halide is present during formation of an organic silver salt (the present invention). In this process an alkali metal soap stably dispersible in water and a water-dispersed silver halide are mixed in water. Therefore, they are readily blended with each other and dispersed without forming aggregation. From this well-dispersed state, the alkali metal soap is converted into an organic silver salt by addition of a water soluble silver salt. Accordingly, this well-dispersed state can be maintained. In the mixture of the silver

halide and the organic silver salt prepared by this type of process, silver halide particles do not aggregate with each other and do not directly contact the organic silver salt, and are observed as a uniform dispersion.

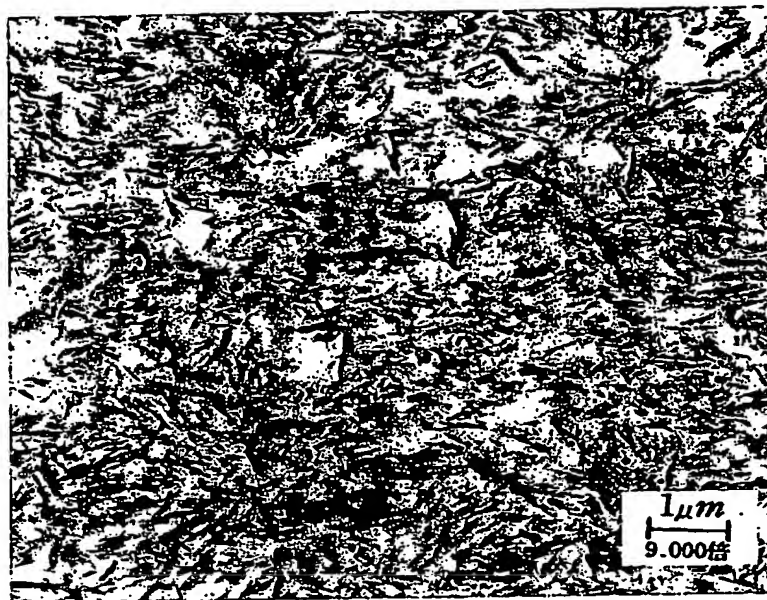


Figure 1. Process in which a preformed silver halide is present during formation of an organic silver salt. Black regions are silver halide and light gray particles are the organic silver salt. It can be seen that the silver halide and the organic silver salt are uniformly dispersed.

Figure 2 shows a dispersion obtained by the conversion process (as described in the Examples of Uytterhoeven). The conversion process partially converts an organic silver salt into a silver halide by reacting the organic silver salt with a halogen ion.

Accordingly, the formed silver halide is coupled to the surfaces of crystals of the organic silver salt, and therefore cannot be dispersed independently from the organic silver salt.



Figure 2: Conversion process. Black portions are silver halide and light gray particles are the organic silver salt. Silver halide is distributed on crystals of the organic silver salt.

As can be seen from the above explanation and photomicrographs, the final products of these two types of dispersions are not the same. Further, the preformed silver halide according to the present invention can be used with conventional particle forming methods to adjust particle size, particle size distribution, halogen composition structure such as core shell and the like, and also can be used with techniques such as metal ion doping and chemical sensitization, whereas none of these techniques can be used with the conversion process (Figure 2).

The secondary reference of EP '310 does not cure the deficiencies of the primary reference. EP '310 teaches the use of silver iodobromide. Such materials are low in iodine, as discussed above. Further, in view of the unexpected results shown in the declaration, it would not have been obvious to use a low-level coating amount of silver in high silver iodide applications.

Claim 16 was rejected over the combination of Uytterhoeven in view of EP '310 and further in view of Tsuzuki. Claim 14 was rejected over the combination of Uytterhoeven in view of EP '310 and further in view of either Goto et al. or Farid et al. None of the tertiary references cure the deficiencies of the primary references. Therefore it is submitted these dependent claims are allowable.

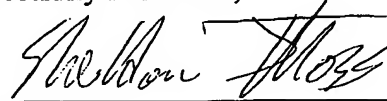
Siga has been used as a secondary reference in some of the rejections. Siga pertains to a post-active type dry image forming material, as recited in the claims thereof, and it is clearly described in the specification that the post-active type dry image forming material is technically different from common dry image forming materials (the photothermographic material of the present invention belongs to this common type). Namely, the dry image forming material of Siga is of a type that is initially not photosensitive, but is rendered photosensitive by heating. A mechanism for accomplishing this change necessitates a combination of constituent features (d) and (e) of claim 1. In contrast, common dry image forming materials are photosensitive from the initial state, and do not use the above combination of the special features (d) and (e). Accordingly, the knowledge provided by Siga does not apply to the photothermographic materials as described in the present application, and therefore, nothing is suggested by Siga. Accordingly, Siga is not an appropriate reference.



Claims 1, 3, 7-9, and 16-18 were provisionally rejected for double patenting. Original claim 12 was not included in this rejection. Since the limitations of claim 12 have been incorporated into claim 1, it is respectfully submitted that this rejection has been overcome.

In view of the foregoing amendments and remarks, it is respectfully submitted that all the claims in the application are in condition for allowance. Early and favorable action is respectfully requested.

Respectfully submitted,



Sheldon Moss  
Reg. No. 52,053

Taiyo, Nakajima & Kato  
401 Holland Lane #407  
Alexandria, VA 22314  
(703) 838-8013  
Date:

*November 28, 2005*

FOURTH EDITION EDITED BY

**T. H. James**

Research Laboratories  
Eastman Kodak Company

SECTION EDITORS

**J. F. Hamilton**

**G. C. Higgins**

**J. E. Starr**

CONTRIBUTORS

**R. K. Ahrenkiel**

**J. H. Altman**

**R. E. Bacon**

**R. C. Baetzold**

**C. R. Berry**

**S. Boyer**

**P. Broadhead**

**E. R. Brown**

**D. M. Burness**

**F. R. Clapper**

**G. M. Corney**

**J. J. DePalma**

**L. Erickson**

**G. C. Farnell**

**L. J. Fleckenstein**

**J. Gasper**

**P. B. Gilman, Jr.**

**J. F. Hamilton**

**J. M. Harbison**

**A. H. Herz**

**D. W. Heseltine**

**P. J. Hillson**

**L. M. Kellogg**

**P. Kowaliski**

**M. A. Kriss**

**W. E. Lee**

**G. I. P. Levenson**

**F. Moser**

**C. N. Nelson**

**J. F. Padday**

**A. Pailliotet**

**J. Pouradier**

**P. I. Rose**

**A. E. Saunders**

**H. E. Spencer**

**H. R. Splettstosser**

**K. H. Stephen**

**D. M. Sturmer**

**J. R. Thirtle**

**L. K. J. Tong**

**E. A. Trabka**

**W. West**

THE  
THEORY  
OF THE  
PHOTOGRAPHIC  
PROCESS  
FOURTH EDITION

Macmillan Publishing Co., Inc.

NEW YORK

Collier Macmillan Publishers

LONDON

COPYRIGHT © 1977, MACMILLAN PUBLISHING CO., INC.  
PRINTED IN THE UNITED STATES OF AMERICA

All rights reserved. No part of this book may be reproduced or transmitted in any form or by any means, electronic or mechanical, including photocopying, recording, or any information storage and retrieval system, without permission in writing from the Publisher.

Earlier editions copyright 1942 and 1954 and copyright © 1966 by Macmillan Publishing Co., Inc.

Macmillan Publishing Co., Inc.  
866 Third Avenue, New York, New York 10022

Collier Macmillan Canada, Ltd.

Library of Congress Cataloging in Publication Data

Main entry under title:

The Theory of the photographic process.

First and 2nd editions edited by C. E. K. Mees.

Includes bibliographical references and indexes.

1. Photography. I. James, Thomas Howard, (date)

II. Mees, Charles Edward Kenneth, 1882-1960. The theory of the photographic process.

TR200.M4 1977 770 76-25432  
ISBN 0-02-360190-6

PRINTING 1 2 3 4 5 6 7 8 YEAR: 7 8 9 0 1 2 3

## CHAPTER

## 1

## PROPERTIES OF SILVER HALIDES

## I. STRUCTURE AND THERMODYNAMIC PROPERTIES

J. POURADIER, A. PAILLIOTET, AND C. R. BERRY

SEVERAL IMPORTANT properties of silver halide crystals have made them the dominant photosensitive material in photographic processes for more than a century. During this time, technological improvements in sensitivity have usually preceded scientific understanding of the underlying phenomena. However, in recent years much more detailed understanding of the photographic process has resulted from investigations in the whole realm of crystal physics, especially from the research on semiconductors and on alkali halides.

One respect in which the silver halides in practical systems differ from most of the other solid-state devices is that they are in the form of very small crystals suspended in a polymer matrix. For this reason much of the literature on crystal growth and imperfections, which usually deals with large crystals, is not directly applicable to the silver halides as used in photographic systems. However, effective methods have been devised for studying the growth and imperfections of microcrystals of the silver halides. Progress along these lines will be described subsequently, but first we shall consider the structure of ideal crystals of the silver halides.

## A. Crystal Structures of Silver Halides

Soon after the discovery of the method of applying x-ray diffraction to the analysis of the structures of

powdered crystalline materials, Wilsey<sup>1</sup> applied it to the silver halides. In 1921 and during the following few years, he established that silver bromide, AgBr, and silver chloride, AgCl, had the rock salt structure and formed solid solutions in all proportions when crystallized by cooling from the melt. The lattice parameter was found to vary as a linear function of composition of the solid solution. Wilsey also determined that silver iodide, AgI, crystallized in either the hexagonal, wurtzite structure ( $\beta$ -AgI) or in the cubic zinc blende structure ( $\gamma$ -AgI), depending on the details of the crystallization process. It was found that, on cooling from the melt, as much as 60 mole % iodide could be incorporated in the silver bromide structure (Figure 1.1) before a second phase having the silver iodide structure appeared.

According to the conclusions of Kolkmeijer and Van Hengel,<sup>2</sup> which have been widely accepted, more nearly cubic AgI is precipitated when silver ions are in excess and more nearly hexagonal AgI when iodide ions are in excess. More recent measurements<sup>3</sup> indicate that the presence or absence of gelatin and the rate of addition of the reactants have pronounced effects on the amounts of cubic and hexagonal AgI. Entirely hexagonal material was produced only when gelatin was present and the solutions were added slowly without an excess of either  $\text{Ag}^+$  or  $\text{I}^-$ . No

TABLE 1.0  
Structure of Silver Halide Crystals

	AgCl	AgBr	AgI			
			$\beta$	$\gamma$	$\alpha$	$\delta$
Structure	face centered cubic rock salt type	face centered cubic rock salt type	hexagonal wurtzite type	face centered cubic zinc-blende type	body centered cubic	face centered cubic rock salt type
Space group	Fm3m	Fm3m	P6 <sub>3</sub> mc	F43m	Im3m	Fm3m
Conditions of formation	are normally formed under the conditions of the photographic emulsion precipitation				above 146° C	above 3–4kbar

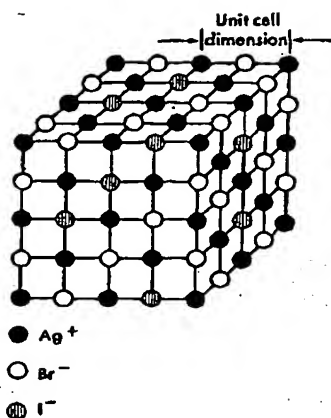


FIG. 1.1. A schematic representation of a random solid solution of AgI in AgBr, where 25% of the bromide-ion sites are occupied by iodide ions.

condition was found where only cubic material was observed.

When AgI is heated above 146°C, it undergoes a solid phase transition accompanied by a remarkable increase in ionic conductivity. The high temperature structure was described by Strock<sup>4</sup> as consisting of iodide ions in a body-centered cubic arrangement, with the silver ions not localized but occupying the large interstitial volumes between iodide ions. Byerley and Hirsch<sup>5</sup> made precipitates of AgI in gelatin at 70°C that contained the metastable high temperature phase, but only when prepared within two separate, narrow regions of low and high pAg. The bright yellow dispersions obtained in that way changed slowly to the ordinary low-temperature, cream-colored silver iodide when kept at the elevated temperature or instantly when cooled to 27°C or below.

By using high energy electrons (40 kV) reflected from the surfaces of single crystals of AgBr, Berry<sup>6</sup> observed that highly oriented, epitaxial AgI containing both hexagonal and cubic structures stacked in random sequence were present whenever the surface had been in contact with solutions of sensitizing-dye cations containing the iodide counter ion. Thus the iodide counter ion in sensitizing dyes must be avoided if one wishes to prevent recrystallization of the surfaces of AgBr crystals.

Alkali halide crystals may be considered with reasonable accuracy to be built from ions that pack together like hard spheres. One value of sphere radius for each metal ion and for each halide ion allows the observed values of lattice dimension for most alkali halide crystals to be well represented according to the relation  $\alpha_{mx} = 2r_m + 2r_x$ , where  $\alpha_{mx}$  is the lattice dimension and  $r_m$  and  $r_x$  are the alkali ion and halide ion radii, respectively. Tables of ionic radii, such as that given by Pauling,<sup>7</sup> which are useful with the alkali

## CH. 1. PROPERTIES OF SILVER HALIDES

halides, do not apply at all to the silver halides. For example, with  $r_{Ag}$  equal to 1.26 Å and  $r_{Br}$  equal to 1.95 Å, the value of the lattice parameter should be 6.42 Å for AgBr. This is much larger than the measured value,<sup>8</sup> 5.77475 Å. The hard-sphere model does not apply accurately to the silver halides because the bonding is not strictly ionic.

To take account of the partially covalent nature of the bonds in silver halides, Van Vechten and Phillips<sup>9</sup> proposed effective radius values of 1.541 Å for silver and 1.343 Å for bromide. Such values are difficult to reconcile with the observations in AgBr that interstitial silver ions are found in unusually high concentrations, but there are no interstitial bromide ions. Moreover, since the substitution of sodium ions (radius 0.97 Å) for silver ions in either AgBr or AgCl swells the lattice,<sup>10</sup> the effective silver ion radius appears to be smaller than that of sodium.

### B. Lattice Energy

The energy of the lattice is defined as the energy required to form a gram molecule of the crystal of silver halide from silver ions and halide ions situated at infinite distance from one another. This energy, important in the process of photolysis, cannot be measured directly because nonsolvated ions cannot be isolated in large quantities. It can be obtained indirectly from experimental values by considering possible reactions leading to the formation of the crystal of silver halide, for example, from bromine and silver metal, using the Born-Haber cycle. Values obtained in this way have a considerable range of uncertainty, as reflected in the range of values given in Table 1.1.

Theoretical values have been obtained by Mayer<sup>11</sup> and by Huggins.<sup>12</sup> The two values given for each salt in Table 1.1 correspond to two different hypotheses concerning the radius of repulsion of the ions. The discrepancy between the theoretical values and those obtained from the Born-Haber cycle increases with increasing covalent character of the bonds.

### C. Thermal Properties

As temperature increases, AgCl and AgBr expand, whereas  $\beta$ - and  $\gamma$ -AgI contract. Values for the linear coefficient of expansion,  $dl/dT$ , at 25° are given in Table 1.1. The thermal expansion of  $\alpha$ -AgI, which is stable above 146°C, is positive, unlike the  $\beta$ - and  $\gamma$ -forms and, in spite of the disagreement between the different values attributed to the expansion coefficient of the  $\alpha$ -form (ranging from  $+7.8 \times 10^{-5}$  to  $+2.9 \times 10^{-4}$ ) it is apparent that this coefficient is large compared with the other silver halides.

TABLE 1.1  
Physical Properties of Silver Halides

	AgCl	AgBr	AgI( $\beta$ )
Lattice energy (kcal mole <sup>-1</sup> )			
experimental	-214.8 to -219.8	-210.4 to -216.7	-208.4 to -213.5
theoretical	-204 <sup>a</sup> -205 <sup>b</sup>	-198 -199	-183 -193
Linear coef. of expansion	$3.20 \times 10^{-5}$	$3.37 \times 10^{-5}$	$(-1.6 \text{ to } -2.8) \times 10^{-6}$
Heat capacity			
(25°C) <sup>c</sup>	12.14	12.53	13.00
(100°C) <sup>c</sup>	13.31	13.68	14.81
Melting point (°C)	455	434	557-558
Heats of fusion (extreme values)	2280-4450	2130-2440	860-3180
Heats of fusion (selected values)	2900 <sup>d</sup> 3100 <sup>e</sup>	2320 <sup>d</sup> 2130 <sup>f</sup>	2250 <sup>e</sup>

<sup>a</sup> Reference 11.<sup>b</sup> Reference 12.<sup>c</sup> Calculated from equations given in reference 13.<sup>d</sup> Reference 14.<sup>e</sup> Reference 15.<sup>f</sup> Reference 16.

The heat capacities of the silver halides have been measured by several investigators over a large range of temperature, and empirical equations have been established representing the variation of the molar heat capacity as a function of the temperature. The equations proposed by the various investigators, for example, Kelley,<sup>13</sup> and Carre, Pham, and Rollin,<sup>17</sup> are formally different but, except in the vicinity of the temperature of fusion, are satisfactorily concordant. Values calculated from Kelley's equations are given in Table 1.1 for 25° and 100° C.

Perrot and Fletcher<sup>18</sup> obtained anomalously high specific heats of  $\alpha$ -AgI when the sample was stoichiometric. The values ranged from 18 cal mole<sup>-1</sup>°C<sup>-1</sup> at 150° C to 26 at 400° C. If the sample deviated from stoichiometry by as little as 1 mole % in either direction, however, the specific heat was normal at 12 cal mole<sup>-1</sup>°C<sup>-1</sup> from 150° to 400° C. These results were explained as an order-disorder transition among silver ions and silver ion vacancies on six sublattices in the structure.

## D. Phase Transition

### 1. FUSION

The temperatures of fusion of the three silver halides are known with a relatively good accuracy, and the most probable values are given in Table 1.1. On the other hand, reported values for the heats of fusion are surprisingly disperse, and every choice is a little arbitrary.

Only AgI decomposes appreciably below the melting point. This decomposition can be prevented by the presence of iodine vapor.

## 2. ALLOTROPIC TRANSITION

The heat of transition from  $\beta$ -AgI to  $\gamma$ -AgI is about 100 cal mole<sup>-1</sup> or less.<sup>19</sup> This small value explains the simultaneous formation of the two structures and the influence of the preparation technique on their relative proportions. Published results on the temperature and enthalpy of transition of the  $\beta$  or  $\gamma$  structures into the  $\alpha$  structure are in good agreement, with only one exception, and are as follows: Temperature of transition, 144.6-150° C, one of the highest values being the most probable;  $\Delta H$ , 1415-1500 cal mole<sup>-1</sup> ( $1780 \pm 130$  according to reference 20). According to Chateau,<sup>21</sup> the transition enthalpy from  $\beta$ - or  $\gamma$ -AgI to the face-centered cubic AgI (rock salt type) is about 600-650 cal mole<sup>-1</sup>.

The heat capacity measurements<sup>18</sup> of stoichiometric  $\alpha$ -AgI reveal an order-disorder transition at 430° C, the latent heat of which is  $300 \pm 50$  cal mole<sup>-1</sup>.

## E. Mixed Crystals of Silver Halides

Only under rather limited conditions of precipitation does the composition of the crystals in a mixed-halide emulsion conform to the equilibrium state. Nevertheless, knowledge of the equilibrium state is important to an understanding of precipitation.

Chateau, Moncet, and Pouradier<sup>22</sup> found quite generally that a small amount of one silver halide, when put into solid solution in another, caused the lattice parameter to change linearly with the concentration of the addition, with no change in crystal structure. The relation of the lattice parameter,  $a$  (in Ångström units) to the amount of the addition is given, for solid

solutions of the silver halides\* in the face-centered cubic (Fm3m) structure, by the following equations: For bromochloride at 25° C:

$$a = 5.5502 + 0.002246[\text{Br}]$$

For iodobromide at 25° C:

$$a = 5.7748 + 0.00368[\text{I}]$$

For iodochloride at 25° C:

$$a = 5.5502 + 0.00635[\text{I}]$$

where [Br] and [I] represent the concentrations of bromide and iodide, respectively, in mole percent.

Silver chloride and silver bromide crystallize in the same structure (face-centered cubic, NaCl type) and can exist in all proportions in solid solutions. Owing to the difference in crystal structure of AgI and the other silver halides, however, only limited amounts of solid solution can occur when iodide is present. The maximum amount of iodide that can exist in solid solution in AgBr depends on the temperature of formation of the crystals and on the conditions of their formation. For crystals prepared very slowly in order to get thermodynamic equilibrium at every stage of their preparation,<sup>23</sup> the maximum amount of iodide is related to the temperature of precipitation  $t$  in °C by the relation:

$$I_{\text{sat}} (\text{in mole } \%) = 31.2 + 0.165(t - 25) \quad (1.1)$$

Supersaturated crystals are sometimes obtained during photographic emulsion preparation<sup>24,25</sup> and, according to Hirsch,<sup>25</sup> crystals precipitated in the presence of gelatin with an excess of alkali halide can contain up to

$$I_{\text{max}} (\text{in mole } \%) = 34.5 + 0.165(t - 25) \quad (1.2)$$

The temperature coefficient is the same in both cases, that is, the supersaturation is independent, or almost independent, of the temperature.

Only much smaller amounts of bromide and chloride can be incorporated in the  $\beta$ -AgI structure (P6<sub>3</sub>mc).<sup>26</sup>

## 1. THERMODYNAMICS OF SILVER CHLOROBROMIDES

Calorimetric and potentiometric methods have been used to study the thermodynamic properties of solid solutions of the silver halides. Eastman and Milner<sup>27</sup> showed that the formation of a 27-73% chlorobromide mixed salt involves a slightly endothermic

\* When referring to mixed silver halide crystals, the convention used is to name the major halide component last. Thus, the designation "silver iodobromide" implies that the crystals are predominantly silver bromide but contain iodide incorporated in the silver bromide structure.

## CH. 1. PROPERTIES OF SILVER HALIDES

reaction (81 cal mole<sup>-1</sup>) and consequently the solid solution is not ideal. However, the measured increase in entropy at 298° K was 1.12 cal mole<sup>-1</sup>°K<sup>-1</sup>, which is almost exactly equal to the ideal value,

$$R(X_{\text{AgCl}} \ln X_{\text{AgCl}} + X_{\text{AgBr}} \ln X_{\text{AgBr}}) = 1.16 \quad (1.3)$$

where  $R$  is the gas constant and  $X_{\text{AgX}}$  is the mole fraction of the components. This proves that the chloride and bromide ions are distributed at random in the solid with neither short- nor long-range order.

The free energy of formation of the mixed crystals is always small.<sup>28</sup> It attains a maximum value of 330 cal mole<sup>-1</sup> for the 50-50 composition. This explains why mixtures of AgBr and AgCl react only very slowly in the dry state at room temperatures.

## 2. THERMODYNAMICS OF SILVER IODOBROMIDES

Unlike the components of the chlorobromide system, silver bromide and silver iodide do not crystallize in the same structure when prepared under the conditions of precipitation of the photographic emulsion. Iodide ions that are incorporated in the rock salt type lattice of the silver iodobromide crystals are kept in a structure that would be unstable in the absence of bromide.

Rock salt type cubic AgI is stable under pressure (>3 kbar)<sup>29,30</sup> and crystallographic studies have shown that silver iodobromides behave as if they were mixed crystals of AgBr and the high pressure AgI structure.<sup>31</sup> They follow Vegard's law; this property implies that the solid solutions are strictly regular with reference to AgBr and AgI in the face-centered cubic structure, and the change in entropy is identical with that of ideal solutions. In practice, mixed crystals are always formed from  $\beta$ (P6<sub>3</sub>mc) or  $\gamma$ (F43m) AgI and it is necessary to take account of the transformation energy in going from  $\beta$ - or  $\gamma$ -AgI to the rock salt type structure.

Whatever the composition, the free energy of formation of mixed silver iodobromide crystals is less than 200 cal mole<sup>-1</sup>; hence, the variation of energy that accompanies the transformation of any system is always very small.<sup>32</sup> For instance, the reorganization of highly supersaturated mixed crystals would liberate only a few calories per mole and this explains why crystals with high iodide content formed at elevated temperatures can subsist for a long time when they are returned to room temperature. Their recrystallization is frequently imperceptible after several years of storage in the dark, and, when a phase transformation occurs, it gives rise to normally saturated crystals or to undersaturated crystals.<sup>33</sup> This last behavior is not clearly understood.



## Sec. IV.B Optical Absorption

interaction is to view the carrier plus the "cloud" of polarization surrounding it as a quasiparticle, called a **polaron**. The strength of the electron-lattice interaction is implicit in the effective mass and mobility of the polaron. The polaron picture is particularly relevant in the silver halides because of their strong polar character, and these materials have served as models for the study of polaron motion in solids.<sup>10</sup>

### B. Optical Absorption

#### 1. PURE CRYSTALS

Optical absorption of AgCl and AgBr of both fundamental and photographic interest begins in the visible and rises to very high values through the ultraviolet spectral region. The absorption spectrum depends strongly on the particular halide, and is also dependent upon temperature and the presence of impurities. In large crystals, absorption coefficients\* as low as  $10^{-2} \text{ cm}^{-1}$  and as high as  $10^6 \text{ cm}^{-1}$  have been measured, and have required a variety of techniques and samples. Transmission studies on large crystals were reported as early as 1920 by Slade and Toy.<sup>11</sup> Fesefeldt and Gyulai,<sup>12</sup> Tutihasi,<sup>13</sup> and Koester and Givens<sup>14</sup> examined evaporated layers, thereby extending the results to higher absorption coefficients. Okamoto<sup>15</sup> determined the absorption over a very broad range by studying large crystals, sheet crystals, and evaporated layers at various temperatures.

Over the years, many people have studied the absorption of the silver halides in selected spectral and temperature ranges, and with varying degrees of spectral resolution dictated by their particular interest. Urbach<sup>16</sup> and Moser<sup>17</sup> examined the temperature dependence of the relatively weak absorption edge in large single crystals of high purity. Their interest centered on the shape of the absorption edge, its relationship to photographic sensitivity, and the effect of impurities on the absorption edge. By studying this absorption edge in finer spectral detail and at temperatures down to 2° K, Brown<sup>18</sup> confirmed the indirect phonon-assisted nature of the transitions involved and was able to determine the energies of the participating phonons. Kanzaki and Sakuragi<sup>19,20</sup> and Joesten and Brown<sup>21</sup> have reported detailed spectra of this phonon-assisted region both in pure AgCl and AgBr and in mixed crystals of Ag(Cl, Br), Ag(I, Br), and Ag(I, Cl). A much more detailed study of this spectral

feature has been reported by Carrera and Brown,<sup>22</sup> who used very carefully annealed thin films. They correlated the experimentally observed peaks with theoretical work on the band structure of the silver halides carried out by Bassani *et al.*,<sup>23</sup> Scop,<sup>24</sup> and Fowler.<sup>25</sup> Carrera and Brown<sup>22</sup> extended measurements to the extreme ultraviolet and were able to make assignments of new spectral features that were consistent with the earlier band structure calculations. Restricting himself to room temperature, White<sup>26</sup> determined the optical constant of large silver halide crystals in the vacuum ultraviolet region by applying a Kramers-Kronig analysis to reflectivity spectra, and Bauer<sup>27</sup> *et al.* recently reported a correction of some systematic errors in that work. Aust,<sup>28</sup> and Brothers and Lynch<sup>29</sup> have studied the effect of pressure on absorption and related the observations to the calculated band structure. Aust's work allows predictions about the position of the absorption edge in mixed silver halide crystals.

In total, these studies have led to a satisfactory understanding of the main features of the optical absorption of the silver halides. Figure 1.16 shows composite spectra, based on many of the cited references, of AgCl and AgBr crystals at room temperature. The spectra range over seven orders of magnitude in absorption coefficient. Limited data on Ag(Br, Cl) and Ag(I, Br) crystals are included in this figure.

For the pure AgCl and AgBr crystals, such a logarithmic plot reveals two dominant regions: (1) a region of strong absorption ( $\alpha \geq 10^4 \text{ cm}^{-1}$ ) related to direct transitions and excitons, and (2) a region of

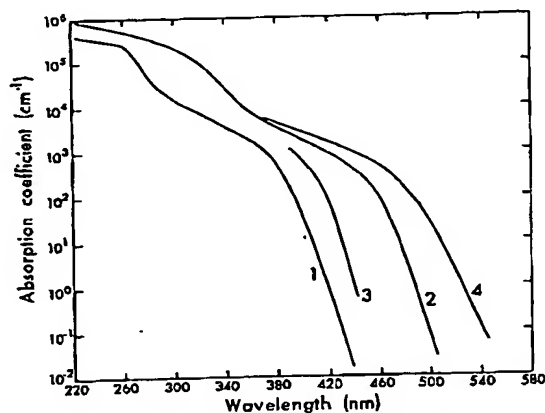


FIG. 1.16. Optical absorption spectrum of pure and mixed silver halide crystals at about 293° K. (1) Pure AgCl; (2) pure AgBr; (3) AgCl containing 10 mole % AgBr; (4) AgBr containing 3 mole % AgI. The AgCl and AgBr spectra are a composite of data on large crystals, thin sheet crystals, and evaporated layers from references noted in the text. The mixed-crystal spectra have not been reported elsewhere.

\*The absorption coefficient ( $\alpha$ ) is defined as the fractional decrease of transmitted light intensity, due to absorption, per unit thickness. Its determination from transmission studies may be complicated by the difficulty of separating reflective and scattering losses from true absorptive loss. It is related to the optical constant,  $\kappa$ , by the relation  $\alpha = 4\pi\kappa/\lambda$ , where  $\lambda$  is the wavelength of the incident light.

weak absorption ( $\alpha < 10^4 \text{ cm}^{-1}$ ) related to indirect phonon-assisted transitions.

The region of strong absorption for AgCl and AgBr at various temperatures is shown on a linear plot in Figure 1.17. The chloride has a pronounced peak at 5.10 eV and a shoulder near 5.20 eV, and the bromide has an intense peak at 4.25 eV with the next peak at 4.82 eV. These separations are close to the spin-orbit splitting of free halogen atoms in their ground state (Cl, 0.11; Br, 0.45), which suggests that the absorption corresponds to a transition involving a halogen atom. The sharpness of the peaks indicates that the electronic transitions involve the formation of an exciton. Carrera and Brown's<sup>22</sup> results on these exciton bands show them to be even narrower and more intense in carefully annealed layers. At 4.2° K in AgBr, the first exciton line is less than 0.08 eV wide and has a maximum absorption coefficient of  $6 \times 10^5 \text{ cm}^{-1}$ , compared to Okamoto's value<sup>15</sup> of 0.12 eV and  $4 \times 10^5 \text{ cm}^{-1}$ . The lower energy, spin-orbit peak in AgCl is more intense than the higher energy component. Onodera and Toyozawa<sup>30</sup> have shown how these exciton intensities and separations can be explained in terms of electron-hole exchange and spin-orbit interaction. They argue that the reversed intensity ratio is evidence for an extended state or a weakly bound electron and hole. Excitons in the alkali halides are much more localized.<sup>31</sup>

As a consequence of the band structure of the silver halides, the energy required to form an exciton is

greater than the energy required to produce free electrons and holes by an indirect absorption process. It is therefore energetically favorable for the exciton to dissociate into a free electron and hole. The results of photoconductive studies at 77° K in AgCl by Van Heyningen and Brown<sup>32</sup> support this expectation. They found a quantum efficiency for production of free electrons and holes varying between 0.5 and 0.8 in the spectral region from 400 nm to 240 nm. This spans both the direct and indirect absorption region.

AgI also has a strong absorption with features related to the spin-orbit splitting of the iodide. AgI is a complex solid existing in three crystal modifications.<sup>33,34</sup> Above about 420° K it forms a body-centered cubic phase, designated as  $\alpha$ -AgI. Below 420° K, a hexagonal wurtzite-type structure designated as  $\beta$ -AgI and a cubic sphalerite-type structure designated as  $\gamma$ -AgI exist. Several authors have analyzed thin-film spectra of AgI.<sup>12,13,35-40</sup> A room temperature spectrum from the work of Hilsch and Pohl,<sup>35</sup> and measurements by Cardona<sup>40</sup> on both  $\beta$ - and  $\gamma$ -AgI at 4° K are shown in Figure 1.18. The peaks near 420 and 330 nm correspond to a separation of 0.8 eV, which is close to the 0.94 eV spin-orbit splitting of the free iodine atom in the ground state. The splitting of the 420-nm peak and the relative displacement of the  $\beta$  and  $\gamma$  absorption curves are a consequence of the perturbing trigonal field of the hexagonal  $\beta$  structure.

The region of weak absorption ( $\alpha \leq 10^4 \text{ cm}^{-1}$ ) in the silver halides, extending from the visible into the ultraviolet, is of primary photographic interest. The main features of this absorption edge have been interpreted in terms of indirect phonon-assisted transitions. The phonon features are observable at low temperature. At higher temperatures ( $> 100^\circ \text{ K}$ ) and

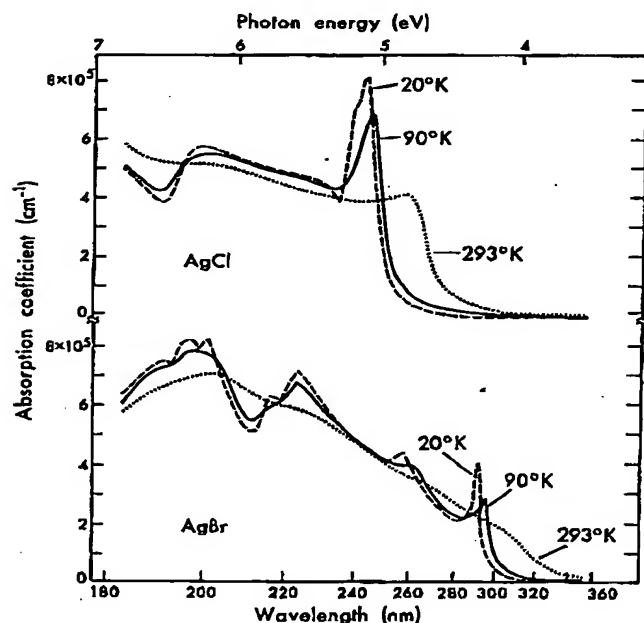


FIG. 1.17. Exciton-region absorption spectrum of AgCl and AgBr evaporated layers at 20, 90, and 293° K. (Reference 15.)

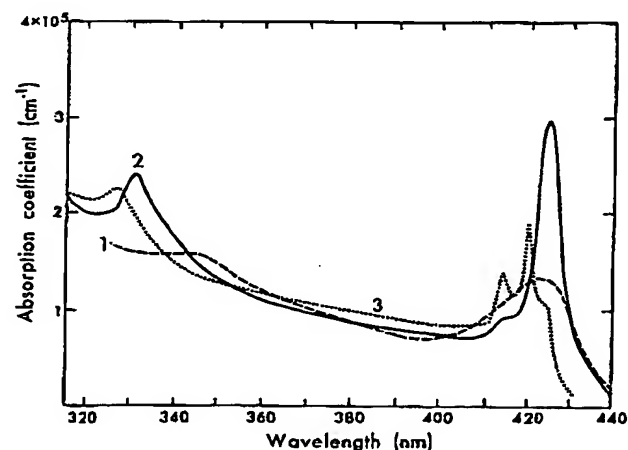


FIG. 1.18. Exciton region absorption spectrum of AgI evaporated layers. (1) AgI at 293° K, uncertain crystal form (reference 35); (2)  $\gamma$ -AgI at 4.2° K (reference 40); (3)  $\beta$ -AgI at 4.2° K (reference 40).

## Sec. IV.B Optical Absorption

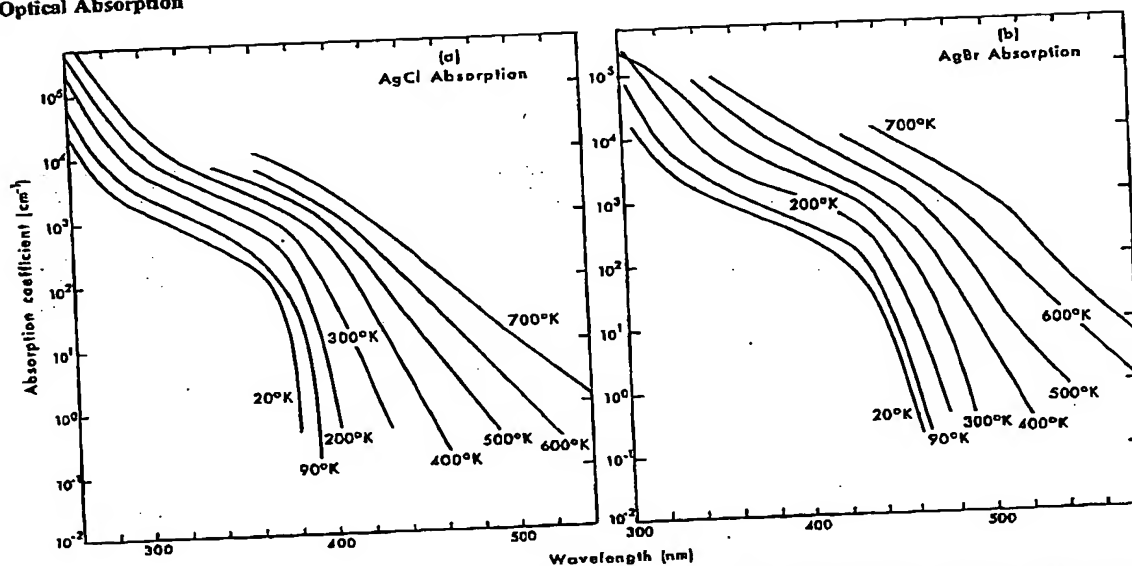


FIG. 1.19. Temperature dependence of the optical absorption edge in AgCl (a) and AgBr (b) crystals. (Reference 15.)

for  $\alpha \leq 10^2 \text{ cm}^{-1}$ , the edge for AgCl and AgBr fits fairly accurately an expression of the form  $\alpha = \alpha_0 \exp[-\sigma(h\nu_0 - h\nu)/kT]$ , where  $h\nu$  is the photon energy and  $T$  the absolute temperature.  $\alpha_0$ ,  $\sigma$ , and  $h\nu_0$  are constants, and  $\sigma$  is about 1 in the silver halides. A closely related derivative form of this dependence was first pointed out by Urbach<sup>16</sup> and has been labeled Urbach's rule. The shape of the absorption edge at room temperature is clearly seen in Figure 1.16, and its dependence on temperature is shown in Figure 1.19. Many people have discussed the origin of such a temperature-dependent exponential absorption edge.<sup>41,42</sup> A theoretical interpretation by Toyozawa and coworkers<sup>43,44</sup> provides both a plausible explanation and a link with the low temperature structure. As temperature increases, they point out, one goes from a range where the edge is determined by the superposition of phonon-assisted processes between well-defined band edges to a high temperature regime where exciton and band processes are smeared out by electric fields associated with the vibrating lattice. Energy-band maxima and minima can still be defined, however, and carrier mobility, trapping, and recombination processes still take place largely as discussed in the context of a static lattice.

The region of weak absorption in AgI has been studied less extensively, perhaps because of anisotropic properties, difficulties in growing good single crystals, and less technological interest. The absorption edges of both  $\alpha$ -AgI and  $\beta$ -AgI have been reported by Suri and Henisch<sup>45</sup> and by Cochrane.<sup>46</sup> A steep edge begins at about 440 nm (arbitrarily defined at about  $10 \text{ cm}^{-1}$ ) and Cochrane<sup>46</sup> has suggested that this edge also arises from indirect phonon-assisted

transitions. There are no reported studies on large crystals of the weak absorption region for the cubic low temperature form ( $\gamma$ -AgI), but the analysis by Berry<sup>38</sup> suggests that the absorption coefficient is about  $5 \times 10^3 \text{ cm}^{-1}$  at 440 nm. Assuming an edge about as steep as the other silver halides, the  $\gamma$ -AgI absorption begins in the 560–580-nm region.

A question of both fundamental and photographic interest is whether silver halide surfaces have absorption properties significantly different from that of the bulk. In principle, such a difference exists as a result of both the intrinsic asymmetry of the surface and the influence of space charge layers and adsorbed impurities. The smoothed curves for AgCl and AgBr shown in Figure 1.16 have been evaluated from overlapping transmission and reflection measurements on large melt-grown crystals, thin sheet crystals ranging from a hundred micrometers to a few micrometers, and evaporated layers less than  $0.5 \mu\text{m}$  thick. Reflection corrections, interference phenomena in thin layers, and errors in thickness determination result in uncertainty in the calculated absolute values of absorption coefficients that can easily be as high as 30%. Within this uncertainty, coefficients obtained on different thin samples are in agreement, but clearly such an uncertainty can mask a fairly strong component of surface absorption different from the bulk. No experimental determination of the surface absorption in thin layers has been reported.

In crystals with dimensions small compared to a tenth of a micrometer there is some published evidence of modified optical properties. Berry<sup>38</sup> has suggested that the exciton absorption in AgI changes in microcrystals of 10 nm, a dimension comparable to

**This Page is Inserted by IFW Indexing and Scanning  
Operations and is not part of the Official Record**

**BEST AVAILABLE IMAGES**

Defective images within this document are accurate representations of the original documents submitted by the applicant.

Defects in the images include but are not limited to the items checked:

- ☐ **BLACK BORDERS**
- ☐ **IMAGE CUT OFF AT TOP, BOTTOM OR SIDES**
- ☐ **FADED TEXT OR DRAWING**
- ☐ **BLURRED OR ILLEGIBLE TEXT OR DRAWING**
- ☐ **SKEWED/SLANTED IMAGES**
- ☐ **COLOR OR BLACK AND WHITE PHOTOGRAPHS**
- ☐ **GRAY SCALE DOCUMENTS**
- ☐ **LINES OR MARKS ON ORIGINAL DOCUMENT**
- ☐ **REFERENCE(S) OR EXHIBIT(S) SUBMITTED ARE POOR QUALITY**
- ☐ **OTHER:** \_\_\_\_\_

**IMAGES ARE BEST AVAILABLE COPY.**

**As rescanning these documents will not correct the image problems checked, please do not report these problems to the IFW Image Problem Mailbox.**